

Upregulation of FGFR1 expression is associated with parathyroid carcinogenesis in HPT-JT syndrome due to an *HRPT2* splicing mutation

Jl-YOUNG LEE¹, SU YEON KIM¹, EUN-YEONG MO¹, EUN-SOOK KIM¹,
JE-HO HAN¹, LEE-SO MAENG², AN-HEE LEE², JUNG WOO EUN³,
SUK WOO NAM³ and SUNG-DAE MOON¹

¹Division of Endocrinology and Metabolism, Department of Internal Medicine, ²Department of Hospital Pathology, Incheon St. Mary's Hospital, The Catholic University of Korea, Bupyeong-gu, Incheon 403-720;

³Department of Pathology, Microdissection Genomics Research Center, College of Medicine, The Catholic University of Korea, Seocho-gu, Seoul 137-701, Republic of Korea

Received March 7, 2014; Accepted April 26, 2014

DOI: 10.3892/ijo.2014.2477

Abstract. Mutations of the *HRPT2* gene, which are responsible for hyperparathyroidism-jaw tumor (HPT-JT) syndrome, have been implicated in the development of a high proportion of parathyroid carcinomas. The aim of this study was to investigate differences in expression of the most important genes connected with parathyroid carcinoma between HPT-JT syndrome due to an *HRPT2* splicing mutation, normal parathyroid tissue and sporadic parathyroid adenoma. Total RNAs were extracted from parathyroid carcinoma in HPT-JT syndrome harbouring *HRPT2* splicing mutation or sporadic parathyroid adenoma and normal parathyroid gland, and subjected to Illumina DASL-based gene expression assay. Unsupervised hierarchical clustering analysis was used to compare gene expression in HPT-JT syndrome, sporadic parathyroid adenoma and normal parathyroid glands. We identified differentially regulated genes in HPT-JT syndrome and sporadic parathyroid adenoma relative to normal parathyroid glands using a combination of Welch's t-test and fold-change analysis. Quantitative PCR, RT-PCR and IHC were used for validation. Sixteen genes differentially regulated in the parathyroid carcinoma were associated with signal pathways, MAPK, regulation of actin cytoskeleton, prostate cancer and apoptosis. *FGFR1* expression was confirmed to be significantly upregulated by validation experiments. Our gene

expression profiling experiments suggest that upregulated *FGFR1* expression appears to be associated with parathyroid carcinoma in HPT-JT syndrome due to an *HRPT2* splicing mutation.

Introduction

Hyperparathyroidism is characterized by calcium-insensitive hyper-secretion of parathyroid hormone and the development of tumors from parathyroid cells. The majority of tumors in primary hyperparathyroidism are sporadic, but ~5% are associated with hereditary cancer syndromes (1). Cases of primary hyperparathyroidism (80-85%) are due to parathyroid adenomas, and 10-15% are attributed to primary chief cell hyperplasia (2).

A molecular analysis of parathyroid hyperplasia, adenoma and carcinoma has been reported (3), and cyclin D1, calcium sensing receptor and vitamin D receptor genes are known to play a role in tumor development in parathyroid glands (4,5). Overexpression of cyclin D1, a key regulator of the cell cycle, has been implicated in the pathogenesis of 20-40% of sporadic parathyroid adenomas (6). In addition, loss of chromosome segment 1p is strongly associated with parathyroid adenoma and carcinoma, but not with hyperplasia (2,3,7,8). Other findings relevant to parathyroid pathogenesis are mutations of the *HRPT2* gene (1q24-32) or *MEN* gene (11q13) (9,10). Germline mutations of the *HRPT2* gene have been described in parathyroid carcinoma, especially in HPT-JT syndrome (11-14), and have been implicated in the development of a high proportion of parathyroid carcinomas (2). Furthermore, microarray profiling has been used to examine different types of parathyroid disease, and these have proved to be excellent objects for understanding the molecular pathogenesis of the parathyroid gland (3,4). However, the molecular events involved in the formation of parathyroid tumors, especially in HPT-JT syndrome, are poorly understood. We therefore generated gene expression profiles of the main types of primary parathy-

Correspondence to: Dr Sung-Dae Moon, Division of Endocrinology and Metabolism, Department of Internal Medicine, Incheon St. Mary's Hospital, The Catholic University of Korea, no. 665 Bupyeong-dong, Bupyeong-gu, Incheon 403-720, Republic of Korea
E-mail: sungdaem@gmail.com

Key words: *HRPT2*, hyperparathyroidism-jaw tumor syndrome, HPT-JT syndrome, parathyroid carcinoma, *FGFR1*

Table I. Clinical and genetic data for the three patients in this study.

Pt	Age (years)	Gender	Ca (mg/dl)	P (mg/dl)	iPTH (pg/ml)	Size (cm)	Wt (gm)	HDx	HRPT2 mutation
KSN	54	Female	9.1	4.3	-	0.3*0.2	-	Normal	None
CJN	57	Female	11.9	2.0	624.28	3.5*2.0	6.0	Sporadic	None
KKT	22	Male	14.1	1.4	1110.51	4.0*2.5	7.5	HPT-JT syndrome	IVS2-1G>A

Pt, patient; Wt, weight; HDx, histologic diagnosis.

roid disease: sporadic parathyroid adenoma, and parathyroid carcinoma in HPT-JT syndrome due to an HRPT2 splicing mutation (hereinafter referred to as HPT-JT syndrome). As a control we also profiled normal parathyroid tissue.

Materials and methods

Tumor samples. Fresh tumor tissues were obtained from the patient with parathyroid tumor in HPT-JT syndrome and one with a sporadic parathyroid tumor (15). As a control, normal parathyroid gland was obtained from excess tissues after routine parathyroid auto-transplantation during thyroidectomy. Sporadic parathyroid adenoma and the parathyroid tumors in HPT-JT syndrome were snap-frozen in liquid nitrogen immediately after surgery and stored at -80°C until use. The parathyroid tumor in HPT-JT syndrome was classified as a carcinoma (15), and confirmed to harbour a germ-line HRPT2 splicing mutation (15,16). The histology of the parathyroid carcinoma was classified according to the WHO guidelines (4). Patient data are summarized in Table I. Approval for this study was obtained from the Human Research Ethics Committees of the participating institutions.

Preparation of RNA. Total RNA was extracted from frozen tissues using TRIzol reagent (Invitrogen Life Technologies, Carlsbad, CA) and purified using Qiagen RNeasy spin columns (Qiagen, Inc., Valencia, CA) according to the protocols recommended by Illumina (San Diego, CA) for DASL applications. After DNase digestion and clean-up procedures, RNA samples were quantified, aliquoted and stored at -80°C until use. For quality control, RNA purity and integrity were evaluated by denaturing gel electrophoresis, OD 260/280 ratio and analysed on an Agilent 2100 Bioanalyzer (Agilent Technologies, Palo Alto, CA).

DASL (cDNA mediated annealing, selection, extension and ligation) assay. A 0.25-1.0 μg samples of total RNA were converted into cDNA using biotinylated random primers, oligo-deoxythymidine primers and Illumina reagents. The resulting biotinylated cDNA was annealed to assay oligonucleotides and bound to streptavidin-conjugated paramagnetic particles to be able to select cDNA/oligo complexes. After oligo hybridization, mis-hybridized and non-hybridized oligos were washed away, and bound oligos were extended and ligated to generate templates for amplification with shared PCR primers. The fluorescence-labelled complementary strand was hybridized at 45°C for 18 h to Illumina HumanRef-8 DASL Expression

BeadChips. After hybridization, the arrays were scanned by laser confocal microscopy using an Illumina BeadArray Reader. Array data export, processing and analysis were performed with Illumina BeadStudio v3.1.3 (Gene Expression Module V3.3.8).

Raw data preparation and statistic analysis. The exported raw array data were filtered by detection P-value <0.05 (similar to noise signals) in at least 50% of samples. We applied a filtering criterion for data analysis in which a higher signal value was required to obtain a detection P-value <0.05 . The selected gene signal value was transformed by logarithm and normalized by a quantile method. Comparisons were carried out using t-tests and Benjamini-Hochberg FDR (false discovery rate) adjusted P-values (<0.05) and fold changes. Subsequently Illumina HumanRef-8 DASL Expression BeadChip expression data were re-analyzed using GenPlex software 3.0 (Istech, Inc., Korea). For primary data filtering, spots with a P-call (detection call P-value <0.1) were selected, and the remaining filtered data were used for further analysis. Quantile normalization was used to normalize data.

Unsupervised and supervised analysis. Unsupervised hierarchical clustering of log ratios was performed with Cluster 3.0, and the results were visualized with Treeview software (Stanford University, Palo Alto, CA). Pearson's correlation, mean centering and average linkage were applied in all clustering applications. For clustering, we used average linkage clustering with standard correlation as the similarity metric. Genes within 0.5 standard deviations of the log-transformed ratios were discarded. To select specific and robust gene sets associated with the normal parathyroid gland, sporadic parathyroid adenoma and HPT-JT syndrome, we used the combination analysis with Welch's t-test and fold-change. On Welch's t-test and fold-change analysis, genes having P-values <0.05 and showing fold-change >2.0 were selected.

KEGG pathway analysis. Molecular pathways associated with differentially expressed genes were identified using the Kyoto Encyclopedia of Genes and Genomes (KEGG) pathway database (<http://www.genome.jp/kegg>). This tool maps genes to known pathways and provides a summary of the biological processes affected. The above tool directs the specific genes to predicted pathways and provides the summary of how the biological processes have been affected. Then, the results of the biological processes were shown by a bar graph, giving the P-value <0.05 that was considered significant in KEGG.

Table II. List of gene-specific primers.

Gene	Primer
FGFR1	F: 5'-CACCCGAGGCATTATTTGAC-3' R: 5'-AAGTTCCTCCACAGGCACAC-3'
FGF19	F: 5'-AGATCAAGGCAGTCGCTCTG-3' R: 5'-CGGATCTCCTCCTCGAAAGC-3'
FGFR2	F: 5'-GACAAAGACAAGCCCAAGGA-3' R: 5'-TGACATAGAGAGGCCCATCC-3'
RELA	F: 5'-TCTGCTTCCAGGTGACAGTG-3' R: 5'-GCCAGAGTTTCGGTTCACCTC-3'
CHUK	F: 5'-GAAGGTGCAGTAACCCCTCA-3' R: 5'-ATTGCCCTGTTCCCTCATTTG-3'
NTRK1	F: 5'-GGACAACCCTTTTCGAGTTCA-3' R: 5'-CAAGGAGCAGCGTAGAAAGG-3'
TCF7	F: 5'-CCTTGATGCTAGGTTCTGGTG-3' R: 5'-GCTTCTTGATGGTTGGCTTC-3'
FGF3	F: 5'-AGATAACGGCAGTGGAGGTG-3' R: 5'-ATTATAGCCAGCTCGTGGA-3'
CACNA1A	F: 5'-AGTGAACAAAAACGCCAACC-3' R: 5'-AAAGTAGCGCAGGTTCAAGGA-3'
FGF22	F: 5'-TTCTACGTGGCCATGAACCG-3' R: 5'-GTGTTGTGGCCGTTCTCTTC-3'
β -actin	F: 5'-GAGCTACGAGCTGCCTGAC-3' R: 5'-GGATGCCACAGGACTCCA-3'
PLCB4	F: 5'-ATCTGGAAGGGCGGATAGTT-3' R: 5'-CATTGGACTGACGTTGTTGG-3'
CAMK2D	F: 5'-AAGGGTGCCATCTTGACAAC-3' R: 5'-TGCTTTCGTGCTTTCACATC-3'
FGF1	F: 5'-TCAGAGGACATGGCAAGGTA-3' R: 5'-GGGAATGTCCCAGGTTAAT-3'
IL1B	F: 5'-TCCAGGGACAGGATATGGAG-3' R: 5'-TCTTTCAACACGCAGGACAG-3'
FGF7	F: 5'-CAGTGGCAGTTGGAATTGTG-3' R: 5'-CCTCCGTTGTGTGTCCATTT-3'
TRAF2	F: 5'-ACCAAGCTGGAAGCCAAGTA-3' R: 5'-GTGAACACAGGCAGCACAGT-3'
MAPK10	F: 5'-CTTCCCAGATTCCCTCTTCC-3' R: 5'-GCTGGGTCATACCAGACGTT-3'
FGF17	F: 5'-CAGATCCGCGAGTACCAACT-3' R: 5'-TCACTCTCAGCCCTTTGAT-3'
FGFR4	F: 5'-TTTCCCCTATGTGCAAGTCC-3' R: 5'-GTAGGAGAGGCCGATGGAAT-3'
CACNA1H	F: 5'-TACTCGTTGGACGGACACAA-3' R: 5'-AAGCACAGCAGAAGGACGTT-3'

Real-time PCR and RT-PCR. First strand cDNA was synthesized using 1 μ g of total RNA, oligo(dT) and SuperScript[®] II Reverse Transcriptase (Invitrogen, Grand Island, NY). RT-PCR was carried out using an iCycler (Bio-Rad, Hercules, CA). The RT-PCR conditions were 95°C for 2 min, followed by 30 cycles at 95°C for 30 sec, 60°C for 30 sec, 72°C for 30 sec and 72°C for 10 min for final extension. Real-time RT-PCR for relevant genes was carried out using a SYBR-Green PCR kit (Bio-Rad) with an Mx3000P™ Real-Time PCR System (Stratagene, La Jolla, CA). The PCR primer sequences used are shown in Table II. The PCR conditions were 95°C for 10 min, followed by 45 cycles of 95°C for 15 sec, 60°C for 1 min and 72°C for 30 sec with a single fluorescence measurement. For dissociation curves, reactions were incubated at 95°C for 1 min, and lamped up from 55 to 95°C at a heating rate of 0.1°C/sec, and fluorescence was measured continuously. Gene expression was calculated according to the 2^{- $\Delta\Delta$ Ct} method using β -actin as an internal standard (17).

Immunohistochemistry (IHC). Tissues were processed for paraffin embedding, and 3- μ m sections were prepared and mounted on glass slides. The mounted sections were pretreated with 10 mM sodium citric acid at 95°C for 10 min for antigen retrieval, and then with 0.3% H₂O₂ in methanol for 30 min to permeabilize them. The sections were blocked using 2.5% horse serum, and then incubated with rabbit anti-FGFR1 antibody (Cell Signaling, Danvers, MA). After rinsing, they were incubated sequentially in biotinylated anti-rabbit antibody and then with ABC complex (Vector, Burlingame, CA) for 1 h at room temperature. Immunoreactivity was visualized by incubation in 3',3'-diaminobenzidine (DAB) solution (Vector) for 50 sec at room temperature. The sections were counterstained with Harris haematoxylin, dehydrated, cleared, mounted and viewed under a light microscope (AX70; Olympus, Tokyo, Japan). For immunofluorescence assays, the mounted sections were blocked with 2.5% horse serum, and incubated with rabbit anti-FGFR1 antibody (Cell Signaling). After rinsing, they were incubated with anti-rabbit antibody. Nuclei were stained with 4',6-diamino-2-phenylindole (DAPI) (ImmunoBioscience, Santa Clara, CA) and viewed under a fluorescence microscopy (Axiovert 200, Carl Zeiss, Oberkochen, Germany).

Results

Transcriptome scans identified large-scale gene expression changes between HPT-JT syndrome, sporadic parathyroid adenoma and normal parathyroid gland. Initially we performed a molecular classification analysis to determine whether our spotted-oligonucleotide microarray system was able to differentiate HPT-JT syndrome, sporadic parathyroid adenoma, and normal parathyroid gland by molecular profiling. We conducted an average linkage unsupervised hierarchical clustering analysis. In Fig. 1A red and green indicate expression levels above and below the median of the sample. We selected 5697 genes (>+2-fold, 3375 and <-2-fold, 2322 genes, P<0.05) in HPT-JT syndrome and 5328 genes (>+2-fold, 3345 and <-2-fold, 1983 genes, P<0.05) in sporadic parathyroid adenoma relative to normal parathyroid gland according to the minimal filtering criteria (Fig. 1B). Venn diagram analysis of gene signatures common to HPT-JT

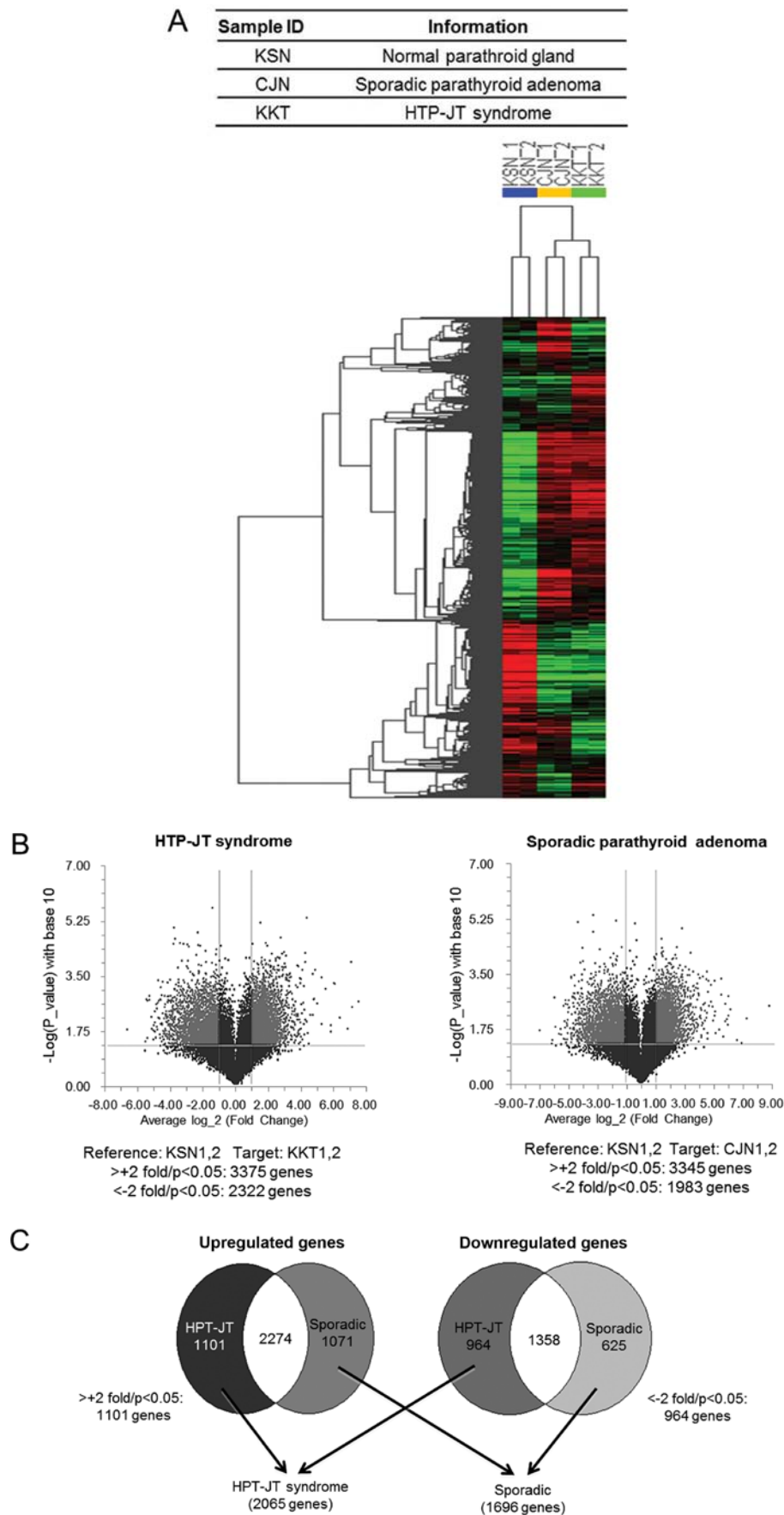


Figure 1. Identification of characteristic molecular signatures of HPT-JT syndrome and sporadic parathyroid adenoma. (A) Dendrogram of unsupervised hierarchical clustering analysis of expression profiling in HPT-JT syndrome, sporadic parathyroid adenoma and normal parathyroid gland. Red and green indicate transcript expression levels respectively above and below the median (black) for each gene across the three study samples. Each sample was duplicated. (B) Two-dimensional clustergram of 5697 genes in HPT-JT syndrome and 5328 genes in sporadic parathyroid adenoma selected relative to the normal parathyroid gland by the minimal filtering criteria. (C) Venn diagram analysis of gene signatures common to HPT-JT syndrome and sporadic parathyroid adenoma, relative to the normal control. The diagram reveals that 2065 genes were de-regulated relative to the normal parathyroid gland in HPT-JT syndrome, and 1696 genes in sporadic parathyroid adenoma.

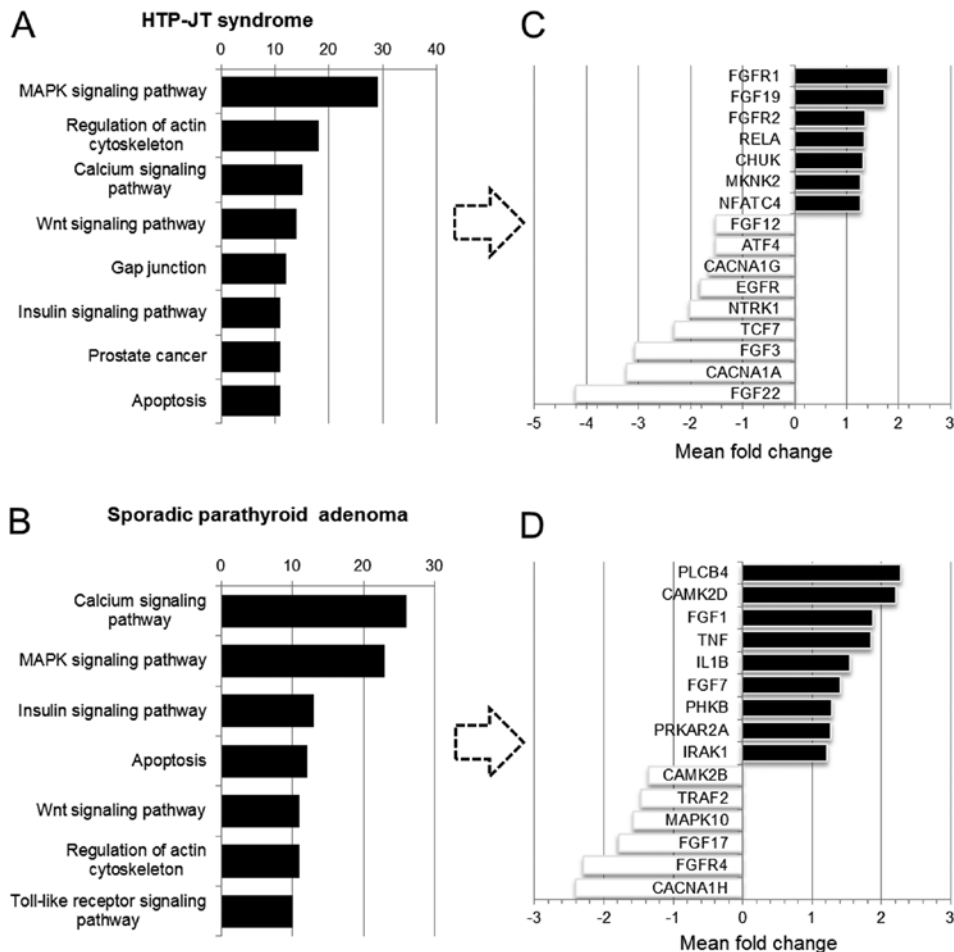


Figure 2. Functional classification of the differentially expressed genes using the KEGG pathway database. The outlier genes in HPT-JT syndrome (A) and in sporadic parathyroid adenoma (B) were classified according to the KEGG pathway to analyse their functions. The bar graph shows the most frequent eight pathways represented. Genes differentially expressed in HPT-JT syndrome (C) and sporadic parathyroid adenoma (D). Solid and open bars represent, respectively, genes differentially up- and downregulated in the two samples. The mean fold changes in gene expression are shown on the x-axis.

syndrome and sporadic parathyroid adenoma revealed that 2065 of the genes were de-regulated relative to the normal parathyroid gland only in HPT-JT syndrome, and 1696 genes only in sporadic parathyroid adenoma (Fig. 1C). These data suggest that thousands of genes either contributed to or were affected by the development of tumor in parathyroid gland.

Identification of molecular signature in HPT-JT syndrome and sporadic parathyroid adenoma. By applying the combination of Welch's t-test and fold-change analysis to the microarray data, we identified an upregulated specific molecular signature of 1101 genes in HPT-JT syndrome, and a downregulated specific molecular signature of 964 genes. Similarly we obtained an upregulated specific molecular signature of 1071 genes in sporadic parathyroid adenoma and a downregulated specific molecular signature of 625 genes. A total of 2274 genes were upregulated in both HPT-JT syndrome and sporadic parathyroid adenoma, and 1358 genes were downregulated in both (Fig. 1C).

Identification of the molecular pathways in HPT-JT syndrome and sporadic parathyroid adenoma. Using the pathway mining tool in the KEGG pathway database we characterized the biological processes in which the 2065 genes in the

HPT-JT syndrome signature and the 1696 genes in the sporadic parathyroid adenoma signature participated (Fig. 2). MAPK, regulation of actin, and calcium signaling pathways were the most significant signaling pathways associated specifically with HPT-JT syndrome (Fig. 2A), while calcium signaling, MAPK and, insulin signaling were the most significant signaling pathways associated with sporadic parathyroid adenoma (Fig. 2B). We sub-classified, according to KEGG, 16 of the genes associated with pathways that were specifically de-regulated in HPT-JT syndrome (Fig. 2C), and 15 of the genes in sporadic parathyroid adenoma (Fig. 2D). In Fig. 2C and D solid and open bars represent genes up- or downregulated, respectively. Genes overexpressed only in HPT-JT syndrome were FGFR1, FGF19, FGFR2, RELA, CHUK, MKNK2 and NFATC4, and genes underexpressed only in HPT-JT syndrome were FGF22, CACNA1A, FGF3, TCF7, NTRK1, EGFR, CACNA1G, ATF4 and FGF12. The PLCB4, CAMK2D, FGF1, TNF, IL1B, FGF7, PHKB, PRKAR2A and IRAK1 were overexpressed only in sporadic parathyroid adenoma, while CACNA1H, FGFR4, FGF17, MAPK10, TRAF2 and CAMK2B were underexpressed. It is evident that the genes de-regulated in HPT-JT syndrome are quite different from those de-regulated in sporadic parathyroid adenoma (Tables III and IV).

Table III. Significant de-regulated pathways and genes associated with HPT-JT syndrome.

KEGG pathway (HPT-JT syndrome)	Genes ^a	P-value
MAPK signaling pathway	FGFR1, FGF19, FGFR2, CHUK, MKNK2, NFATC4 , FGF12, ATF4, CACNA1G, EGFR, NTRK1, FGF3, CACNA1A, FGF22	0
Regulation of actin cytoskeleton	FGFR1, FGF19, FGFR2 , FGF12, EGFR, FGF3, FGF22	9.48E-10
Prostate cancer	FGFR1, FGFR2, RELA, CHUK , ATF4, EGFR, TCF7	2.99E-08
Apoptosis	RELA, CHUK, NTRK1	1.85E-08

Significant de-regulated pathways and genes associated with sporadic parathyroid adenoma.

KEGG pathway (sporadic parathyroid adenoma)	Genes ^a	P-value
Calcium signaling pathway	PLCB4, CAMK2D, PHKB , CAMK2B, CACNA1H	0
MAPK signaling pathway	FGF1, TNF, IL1B, FGF7 , TRAF2, MAPK10, FGF17, FGFR4, CACNA1H	3.51E-14
Insulin signaling pathway	PHKB, PRKAR2A , MAPK10	6.41E-09
Apoptosis	TNF, IL1B, PRKAR2A, IRAK1 , TRAF2	2.09E-10
Wnt signaling pathway	PLCB4, CAMK2D , CAMK2B, MAPK10	1.07E-06
Regulation of actin cytoskeleton	FGF1, FGF7 , FGF17, FGFR4	3.51E-05
Toll-like receptor signaling pathway	TNF, IL1B, IRAK1 , MAPK10	2.45E-07

^aBold character, upregulated genes.

Experimental validation of the molecular signature in HPT-JT syndrome and sporadic parathyroid adenoma using comparative real-time PCR and RT-PCR. In order to validate the gene expression data obtained by the DASL-assay, we selected the genes highly de-regulated in both HPT-JT syndrome and sporadic parathyroid adenoma shown in Fig. 2C and D, and performed comparative real-time reverse transcriptase-PCR analysis and RT-PCR. Levels of transcription of 10 selected genes up- and downregulated in HPT-JT syndrome are shown in Fig. 3A and B, respectively, and those of 10 genes up- and downregulated in sporadic parathyroid adenoma in Fig. 3C and D. Comparative real-time RT-PCR data showed that FGFR1, FGFR2, FGF19, RELA and CHUK were upregulated in HPT-JT syndrome relative to sporadic parathyroid adenoma, in good agreement with the microarray data (Fig. 2C). Similarly NTRK1 and FGF22 were downregulated in agreement with the microarray data, but the findings for TCF7, FGF3, CACNA1A were ambiguous, and their levels of expression were low (Figs. 3B and 4A). In sporadic parathyroid adenoma, the genes for PLCB4, FGF1, IL1B, FGF7, MAPK10, FGFR4 did not differ significantly between the two samples, whereas for CAMK2D, TRAF2, FGF17, CACNA1H the data of real-time PCR and RT-PCR conflicted with the microarray findings (Figs. 3C and D, 4A). The most highly expressed gene in HPT-JT syndrome, FGFR1, was further validated by immunohistochemistry. Immunohistochemical

staining with FGFR1 antibody revealed strong expression in HPT-JT syndrome, but no detectable expression in sporadic parathyroid adenoma or normal parathyroid gland (Fig. 4B). The finding that FGFR1 protein expression was significantly upregulated in HPT-JT syndrome suggests that FGFR1 does indeed play a role in parathyroid carcinogenesis.

Discussion

Parathyroid carcinoma is a rare malignant tumor responsible for less than 1% of cases of hyperparathyroidism. An increased incidence of this carcinoma has been reported in patients with HPT-JT syndrome (2). The incidence of parathyroid carcinoma in HPT-JT syndrome is reported to be as high as 15% (18,19). Germline mutations of the HRPT2 gene have been described in parathyroid carcinoma and in HPT-JT parathyroid carcinoma syndrome (11-14), but the function of the HRPT2 gene is unknown. Previously, we were able to amplify the mutated allele generated by a splice acceptor site mutation of HRPT2 in HPT-JT syndrome (15), and we quantified the aberrantly spliced HRPT2 mRNA resulting from the splicing abnormality by real-time RT-PCR (16). Loss of HRPT2 expression was found to alter the expression of several target genes that are associated with cell growth and cell death (20).

In this study, to clarify the molecular mechanisms involved in the development of parathyroid carcinomas in

Table IV. Genes frequently de-regulated in HPT-JT syndrome.

Unigene	Symbol	Gene name	Fold change ^a	Molecular function
Hs.264887	FGFR1	Fibroblast growth factor receptor 1	1.81	Mitogenesis and differentiation
Hs.249200	FGF19	Fibroblast growth factor 19	1.74	Tumor growth and invasion
Hs.533683	FGFR2	Fibroblast growth factor receptor 2	1.36	Mitogenesis and differentiation
Hs.502875	RELA	v-rel reticuloendotheliosis viral oncogene homolog A (avian)	1.35	Ubiquitous transcription factor
Hs.198998	CHUK	Conserved helix-loop-helix ubiquitous kinase	1.33	Ubiquitination pathway, thereby activating the transcription factor
Hs.515032	MKNK2	MAP kinase interacting serine/threonine kinase 2	1.28	Oncogenic transformation and malignant cell proliferation
Hs.77810	NFATC4	Nuclear factor of activated T-cells, cytoplasmic, calcineurin-dependent 4	1.28	A member of the nuclear factors of activated T cells DNA-binding transcription complex
Hs.584758	FGF12	Fibroblast growth factor 12	-1.50	Regulate cardiac Na(+) and Ca(2+) channel currents
Hs.496487	ATF4	Activating transcription factor 4	-1.50	Encodes a transcription factor
Hs.591169	CACNA1G	Calcium channel, voltage-dependent, T type, α 1G subunit	-1.63	Cell motility, cell division and cell death
Hs.488293	EGFR	Epidermal growth factor receptor	-1.81	Cell proliferation
Hs.406293	NTRK1	Neurotrophic tyrosine kinase, receptor, type 1	-2.00	Cell differentiation
Hs.573153	TCF7	Transcription factor 7 (T-cell specific, HMG-box)	-2.30	Lymphocyte differentiation
Hs.37092	FGF3	Fibroblast growth factor 3	-3.05	Cell growth, morphogenesis, tissue repair, tumor growth and invasion
Hs.501632	CACNA1A	Calcium channel, voltage-dependent, P/Q type, α 1A subunit	-3.21	Hormone or neurotransmitter release and gene expression
Hs.248087	FGF22	Fibroblast growth factor 22	-4.19	Cell growth, morphogenesis, tissue repair, tumor growth and invasion

^aRatio of log₂-transformed mean expression values (HPT-JT syndrome vs. normal parathyroid gland).

Genes frequently de-regulated in sporadic parathyroid adenoma.

Unigene	Symbol	Gene name	Fold change ^a	Molecular function
Hs.472101	PLCB4	Phospholipase C, β 4	2.29	Intracellular transduction of many extracellular signals in the retina
Hs.144114	CAMK2D	Calcium/calmodulin-dependent protein kinase (CaM kinase) II δ	2.22	Alternative splicing results in multiple transcript variants
Hs.483635	FGF1	Fibroblast growth factor 1	1.88	Embryonic development, cell growth, morphogenesis, tissue repair, tumor growth and invasion
Hs.241570	TNF	Tumor necrosis factor	1.86	Cell proliferation, differentiation, apoptosis, lipid metabolism and coagulation
Hs.126256	IL1B	Interleukin 1, β	1.56	Cell proliferation, differentiation and apoptosis
Hs.567268	FGF7	Fibroblast growth factor 7	1.41	Embryonic development, cell growth, morphogenesis, tissue repair, tumor growth and invasion

Table IV. Continued.

Unigene	Symbol	Gene name	Fold change ^a	Molecular function
Hs.78060	PHKB	Phosphorylase kinase, β	1.29	The δ subunit mediates the dependence of the enzyme on calcium concentration
Hs.631923	PRKAR2A	Protein kinase, cAMP-dependent, regulatory, type II, α	1.28	Regulate protein transport from endosomes to the Golgi apparatus and further to the endoplasmic reticulum (ER)
Hs.522819	IRAK1	Interleukin-1 receptor-associated kinase 1	1.23	IL1-induced upregulation of the transcription factor NF- κ B
Hs.351887	CAMK2B	Calcium/calmodulin-dependent protein kinase (CaM kinase) II β	-1.34	Different cellular localizations and interact differently with calmodulin
Hs.522506	TRAF2	TNF receptor-associated factor 2	-1.45	Mediator of the anti-apoptotic signals from TNF receptors
Hs.125503	MAPK10	Mitogen-activated protein kinase 10	-1.56	Proliferation, differentiation, transcription regulation and development
Hs.248192	FGF17	Fibroblast growth factor 17	-1.78	Embryonic development cell growth, morphogenesis, tissue repair, tumor growth and invasion
Hs.165950	FGFR4	Fibroblast growth factor receptor 4	-2.28	Mitogenesis and differentiation
Hs.459642	CACNA1H	Calcium channel, voltage-dependent, T type, α 1H subunit	-2.39	Influx of calcium ions into the cell upon membrane polarization

^aRatio of \log_2 -transformed mean expression values (sporadic parathyroid adenoma vs. normal parathyroid gland).

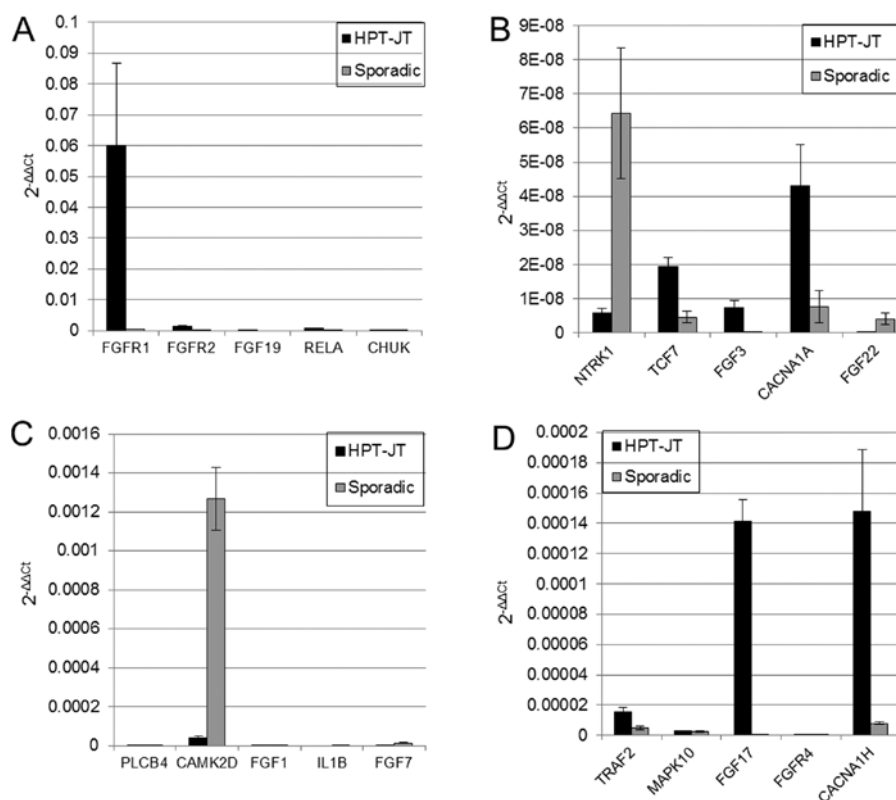


Figure 3. Relative reverse transcriptase-PCR verification. To validate the microarray gene expression data, highly de-regulated genes (A and C, upregulated genes; B and D, downregulated genes) were selected, and relative real-time reverse transcriptase-PCR analysis was performed to validate the microarray data for HPT-JT syndrome and sporadic parathyroid adenoma. Gene expression was calculated by the $2^{-\Delta\Delta C_t}$ method using β -actin as an internal standard. Data are means \pm SDs for triplicate experiments.

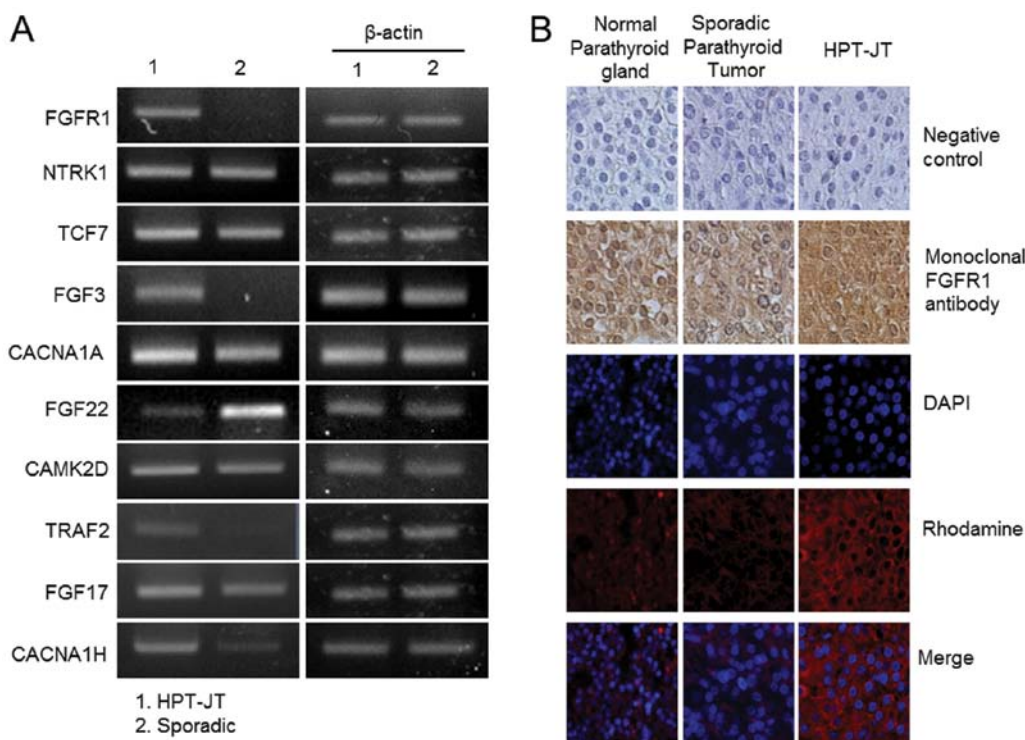


Figure 4. Representative images of FGFR1 immunoreactivity in HPT-JT syndrome, sporadic parathyroid adenoma, and normal parathyroid gland. RT-PCR was also performed on selected genes that were differentially affected in HPT-JT syndrome and sporadic parathyroid adenoma (A). FGFR1 and FGF3 were upregulated, and FGF22 was downregulated in HPT-JT syndrome. Representative immunohistochemistry results for FGFR1 protein expression (B). FGFR1 was highly expressed in HPT-JT syndrome, but barely detectable in sporadic parathyroid adenoma and normal parathyroid gland. Original magnification, x400.

HPT-JT syndrome harbouring a splicing HRPT2 mutation, we undertook gene expression profiling using Illumina DASL matrices. We identified sixteen genes in the HPT-JT syndrome involved in regulation of MAPK signaling, regulation of actin cytoskeleton, prostate cancer and apoptosis pathways, and 15 genes in sporadic parathyroid adenoma involved in calcium signaling, MAPK signaling, insulin signaling, apoptosis and Wnt signaling (Fig. 2, Table III). Our data suggest that increased expression of fibroblast growth factor receptor type 1 (FGFR1) is highly relevant to parathyroid carcinogenesis in HPT-JT syndrome harbouring an HRPT2 splicing mutation. FGF signaling mediated by FGFR involves a classic receptor tyrosine kinase signaling pathway and its de-regulation at various points can result in malignancy (21). FGF signaling is involved in multiple developmental processes including embryonic mesodermal patterning (22). In the adult, it contributes to tissue homeostasis, as well as tissue repair, angiogenesis and inflammation (23,24). Elevated levels of FGFR1 have been found in a number of cancers, including prostate, breast and sarcoma (25-28). One study detected frequent focal amplification of FGFR1 in non-small cell lung carcinoma cell lines, and these cell lines were dependent on FGFR1 activity for growth (29,30). FGFR1 is frequently upregulated in prostate cancer (29,31). Klotho, which is expressed in the kidney, pituitary and parathyroid glands, converts FGFs into a specific receptor for FGF-23 (32,33). The parathyroid cells expressing Klotho and FGFR1 are responsive to FGF-23, both *in vivo* and *in vitro* (33,34). However, studies on FGFR-Klotho signaling in parathyroid glands show

conflicting results (33). One current hypothesis suggests that FGFR1 upregulation destroys the subtle interplay between epithelial and mesenchymal cells (30), and FGFR1 has also been suggested to have tumor suppressor properties, since downregulated expression of FGFR2 in particular has been found in many cancers (21,35-37). However, it is not clear whether FGFR2 is a tumor suppressor, since it is also found to be upregulated in gastric, pancreatic and lung cancers (21). Further studies are necessary to clarify the role of FGFR1 in parathyroid glands. Our results may provide insight into the pathogenesis of parathyroid neoplasia in the HPT-JT syndrome.

In summary, our gene expression profiling experiments suggest that upregulation of FGFR1 expression is associated with parathyroid carcinogenesis in HPT-JT syndrome due to an HRPT2 splicing mutation. Hence FGF signaling molecules may provide useful targets for treatment.

Acknowledgements

This study was supported by Basic Science Research Program through the National Research Foundation of Korea (NRF) funded by the Ministry of Education, Science and Technology (2011-0008886).

References

1. Starker LF, Akerstrom T, Long WD, *et al*: Frequent germ-line mutations of the MEN1, CASR, and HRPT2/CDC73 genes in young patients with clinically non-familial primary hyperparathyroidism. *Horm Cancer* 3: 44-51, 2012.

2. DeLellis RA: Parathyroid carcinoma: an overview. *Adv Anat Pathol* 12: 53-61, 2005.
3. Hunt JL, Carty SE, Yim JH, Murphy J and Barnes L: Allelic loss in parathyroid neoplasia can help characterize malignancy. *Am J Surg Pathol* 29: 1049-1055, 2005.
4. Haven CJ, Howell VM, Eilers PH, *et al*: Gene expression of parathyroid tumors: molecular subclassification and identification of the potential malignant phenotype. *Cancer Res* 64: 7405-7411, 2004.
5. Yano S, Sugimoto T, Tsukamoto T, *et al*: Decrease in vitamin D receptor and calcium-sensing receptor in highly proliferative parathyroid adenomas. *Eur J Endocrinol* 148: 403-411, 2003.
6. Arnold A, Shattuck TM, Mallya SM, *et al*: Molecular pathogenesis of primary hyperparathyroidism. *J Bone Miner Res* 17 (Suppl 2): N30-N36, 2002.
7. Szabo E, Carling T, Hessman O and Rastad J: Loss of heterozygosity in parathyroid glands of familial hypercalcemia with hypercalciuria and point mutation in calcium receptor. *J Clin Endocrinol Metab* 87: 3961-3965, 2002.
8. Valimaki S, Forsberg L, Farnebo LO and Larsson C: Distinct target regions for chromosome 1p deletions in parathyroid adenomas and carcinomas. *Int J Oncol* 21: 727-735, 2002.
9. Cetani F, Pardi E, Giovannetti A, *et al*: Genetic analysis of the MEN1 gene and HRPT2 locus in two Italian kindreds with familial isolated hyperparathyroidism. *Clin Endocrinol (Oxf)* 56: 457-464, 2002.
10. Tanaka C, Uchino S, Noguchi S, *et al*: Biallelic inactivation by somatic mutations of the MEN1 gene in sporadic parathyroid tumors. *Cancer Lett* 175: 175-179, 2002.
11. Cetani F, Pardi E, Borsari S, *et al*: Genetic analyses of the HRPT2 gene in primary hyperparathyroidism: germline and somatic mutations in familial and sporadic parathyroid tumors. *J Clin Endocrinol Metab* 89: 5583-5591, 2004.
12. Hobbs MR, Pole AR, Pidwirny GN, *et al*: Hyperpara-athyroidism-jaw tumor syndrome: the HRPT2 locus is within a 0.7-cM region on chromosome 1q. *Am J Hum Genet* 64: 518-525, 1999.
13. Howell VM, Haven CJ, Kahnoski K, *et al*: HRPT2 mutations are associated with malignancy in sporadic parathyroid tumours. *J Med Genet* 40: 657-663, 2003.
14. Shattuck TM, Valimaki S, Obara T, *et al*: Somatic and germ-line mutations of the HRPT2 gene in sporadic parathyroid carcinoma. *N Engl J Med* 349: 1722-1729, 2003.
15. Moon SD, Park JH, Kim EM, *et al*: A Novel IVS2-1G>A mutation causes aberrant splicing of the HRPT2 gene in a family with hyperparathyroidism-jaw tumor syndrome. *J Clin Endocrinol Metab* 90: 878-883, 2005.
16. Moon S, Kim JH, Shim JY, *et al*: Analysis of aberrantly spliced HRPT2 transcripts and the resulting proteins in HPT-JT syndrome. *Mol Genet Metab* 100: 365-371, 2010.
17. Livak KJ and Schmittgen TD: Analysis of relative gene expression data using real-time quantitative PCR and the 2(-Delta Delta C(T)) method. *Methods* 25: 402-408, 2001.
18. Carpten JD, Robbins CM, Villablanca A, *et al*: HRPT2, encoding parafibromin, is mutated in hyperparathyroidism-jaw tumor syndrome. *Nat Genet* 32: 676-680, 2002.
19. Hewitt KM, Sharma PK, Samowitz W and Hobbs M: Aberrant methylation of the HRPT2 gene in parathyroid carcinoma. *Ann Otol Rhinol Laryngol* 116: 928-933, 2007.
20. Wang P, Bowl MR, Bender S, *et al*: Parafibromin, a component of the human PAF complex, regulates growth factors and is required for embryonic development and survival in adult mice. *Mol Cell Biol* 28: 2930-2940, 2008.
21. Ahmad I, Iwata T and Leung HY: Mechanisms of FGFR-mediated carcinogenesis. *Biochim Biophys Acta* 1823: 850-860, 2012.
22. De Moerlooze L, Spencer-Dene B, Revest JM, Hajihosseini M, Rosewell I and Dickson C: An important role for the IIIb isoform of fibroblast growth factor receptor 2 (FGFR2) in mesenchymal-epithelial signalling during mouse organogenesis. *Development* 127: 483-492, 2000.
23. Turner N and Grose R: Fibroblast growth factor signalling: from development to cancer. *Nat Rev Cancer* 10: 116-129, 2010.
24. Haugsten EM, Wiedlocha A, Olsnes S and Wesche J: Roles of fibroblast growth factor receptors in carcinogenesis. *Mol Cancer Res* 8: 1439-1452, 2010.
25. Kwabi-Addo B, Ozen M and Ittmann M: The role of fibroblast growth factors and their receptors in prostate cancer. *Endocr Relat Cancer* 11: 709-724, 2004.
26. Freier K, Schwaenen C, Sticht C, *et al*: Recurrent FGFR1 amplification and high FGFR1 protein expression in oral squamous cell carcinoma (OSCC). *Oral Oncol* 43: 60-66, 2007.
27. Meyer KB, Maia AT, O'Reilly M, *et al*: Allele-specific up-regulation of FGFR2 increases susceptibility to breast cancer. *PLoS Biol* 6: e108, 2008.
28. Jacquemier J, Adelaide J, Parc P, *et al*: Expression of the FGFR1 gene in human breast-carcinoma cells. *Int J Cancer* 59: 373-378, 1994.
29. Murphy T, Darby S, Mathers ME and Gnanapragasam VJ: Evidence for distinct alterations in the FGF axis in prostate cancer progression to an aggressive clinical phenotype. *J Pathol* 220: 452-460, 2010.
30. Acevedo VD, Gangula RD, Freeman KW, *et al*: Inducible FGFR-1 activation leads to irreversible prostate adenocarcinoma and an epithelial-to-mesenchymal transition. *Cancer Cell* 12: 559-571, 2007.
31. Armstrong K, Ahmad I, Kalna G, *et al*: Upregulated FGFR1 expression is associated with the transition of hormone-naïve to castrate-resistant prostate cancer. *Br J Cancer* 105: 1362-1369, 2011.
32. Urakawa I, Yamazaki Y, Shimada T, *et al*: Klotho converts canonical FGF receptor into a specific receptor for FGF23. *Nature* 444: 770-774, 2006.
33. Imanishi Y, Nagata Y and Inaba M: Parathyroid diseases and animal models. *Front Endocrinol (Lausanne)* 3: 78, 2012.
34. Ben-Dov IZ, Galitzer H, Lavi-Moshayoff V, *et al*: The parathyroid is a target organ for FGF23 in rats. *J Clin Invest* 117: 4003-4008, 2007.
35. Amann T, Bataille F, Spruss T, *et al*: Reduced expression of fibroblast growth factor receptor 2IIIb in hepatocellular carcinoma induces a more aggressive growth. *Am J Pathol* 176: 1433-1442, 2010.
36. Diez de Medina SG, Chopin D, El Marjou A, *et al*: Decreased expression of keratinocyte growth factor receptor in a subset of human transitional cell bladder carcinomas. *Oncogene* 14: 323-330, 1997.
37. Naimi B, Latil A, Fournier G, Mangin P, Cussenot O and Berthon P: Down-regulation of (IIIb) and (IIIc) isoforms of fibroblast growth factor receptor 2 (FGFR2) is associated with malignant progression in human prostate. *Prostate* 52: 245-252, 2002.